Carbohydrate Polymers 98 (2013) 358–365

Contents lists available at SciVerse ScienceDirect

Carbohydrate Polymers

journal homepage: www.elsevier.com/locate/carbpol

Synthesis of CarAlg/MMt nanocomposite hydrogels and adsorption of cationic crystal violet

Gholam Reza Mahdavinia[a,*], Huriyeh Aghaie[b], Hossein Sheykhloie[c], Mohammad Taghi Vardini[b], Hossein Etemadi[a]

[a] Department of Chemistry, Faculty of Science, University of Maragheh, P.O. Box 55181-83111, Maragheh, Iran
[b] Department of Applied Chemistry, Faculty of Science, Tabriz Branch, Islamic Azad University, P.O. Box 1655, Tabriz, Iran
[c] Department of Chemistry, Faculty of Science, Maragheh Branch, Islamic Azad University, P.O. Box 345, Maragheh, Iran

ARTICLE INFO

Article history:
Received 28 January 2013
Received in revised form 30 May 2013
Accepted 31 May 2013
Available online 18 June 2013

Keywords:
kappa-Carrageenan
Sodium alginate
Nanocomposite
Hydrogel
Adsorption

ABSTRACT

CarAlg/MMt nanocomposite hydrogels composed of *kappa*-carrageenan (Car) and sodium alginate (Alg) biopolymers were synthesized by incorporation of sodium montmorillonite (Na-MMt) nanoclay. Acrylamide (AAm), methylenebisacrylamide (MBA), and ammonium persulfate (APS) were used as monomer, crosslinker, and initiator, respectively. The structure and morphology of nanocomposites were characterized by XRD, SEM, and TEM techniques. The XRD results showed exfoliated MMt nanoclay and exfoliation of MMt was confirmed by TEM graph. The resulting nanocomposites were evaluated to remove cationic crystal violet (CV) dye from water. According to data, the adsorption capacity of nanocomposites was enhanced as the clay content was increased. The experimental data were analyzed according to both Langmuir and Freundlich models and experimental maximum adsorption capacity was obtained 88.8 mg g^{-1}. By studying the effect of pH on the dye adsorption capacity of nanocomposites, it was revealed that the adsorption capacity of nanocomposites was enhanced at acidic pHs as the Na-MMt nanoclay and *kappa*-carrageenan components were increased.

1. Introduction

Alginates and carrageenans are renewable resources on earth. These biopolymers are known as polyanionic biomaterials carrying sulfate ($-OSO_3^-$, carrageenans) and carboxylate ($-CO_2^-$, alginates) groups (Mohamadnia, Zohuriaan-Mehr, Kabiri, Jamshidi, & Mobedi, 2008). Because of environmental-friendly, biodegradability, and non-toxicity properties, there are considerable attentions to develop new applicable materials from these biopolymers. Healthcare, pharmaceutical, and water treatment are the important industries in the use of these biopolymers (Crini, 2005; Datta, Mody, Gopalsamy, & Jha, 2011; Goh, Heng, & Chan, 2012; Pawar & Edgar, 2012). Sodium alginate, a water-soluble salt of alginic acid, is a natural linear polysaccharide from marine brown algae composed of β-D-mannuronic and α-L-guluronic acid residues arranged in a nonregular and block-wise fashion along the chain (Bajpai & Tankhiwale, 2006). *kappa*-Carrageenan comprises a family of linear water-soluble sulfated polysaccharides extracted from red seaweeds that have the ability to form thermoreversible hydrogels and are extensively used as gelling agent in food and pharmaceutical industries (Piculell, 1995). Fig. 1 represents the structure of *kappa*-carrageenan and sodium alginate.

Hydrogels are three-dimensional crosslinked polymers containing hydrophilic groups which able to absorb water (Omidian, Rocca, & Park, 2005). Because of specific properties of hydrogels, they have useful application such as drug delivery, tissue engineering, metal ions and biomolecules separation (Dragan, Perju, & Dinu, 2012; Nair & Laurencin, 2007; Tang et al., 2010). The hydrogels from alginate and carrageenan have been synthesized and studied (Hosseinzadeh, Pourjavadi, Mahdavinia, & Zohuriaan-Mehr, 2005; Nochos, Douroumis, & Bouropolos, 2008; Pourjavadi, Barzegar, & Mahdavinia, 2006). Hydrogels can classify into non-ionic and ionic materials. The ionic types comprise anionic ($-CO_2^-$, $-SO_3^-$) or cationic pendants ($-NR_3^+$). The presence of these ionic groups in the hydrogels opens potential area of application that is related to remove pollutants from wastewaters (Shen, Shen, Wen, Wang, & Liu, 2011). Industry is a huge source of water pollution; it produces pollutants that are excessively harmful to people and the environment. Colored water and solutions containing toxic heavy metals and dyes from many industries like dye, textile, paper, plastic, plating, and mining facilities produce considerable polluted waters. The pollutions must be removed from wastewater before discharging it into the environment. Adsorption process, an inexpensive and simple design, can be used to remove of dye contaminations from

* Corresponding author. Tel.: +98 421 227 6060; fax: +98 421 227 6060.
E-mail address: grmnia@maragheh.ac.ir (G.R. Mahdavinia).

0144-8617/$ – see front matter © 2013 Elsevier Ltd. All rights reserved.
http://dx.doi.org/10.1016/j.carbpol.2013.05.096

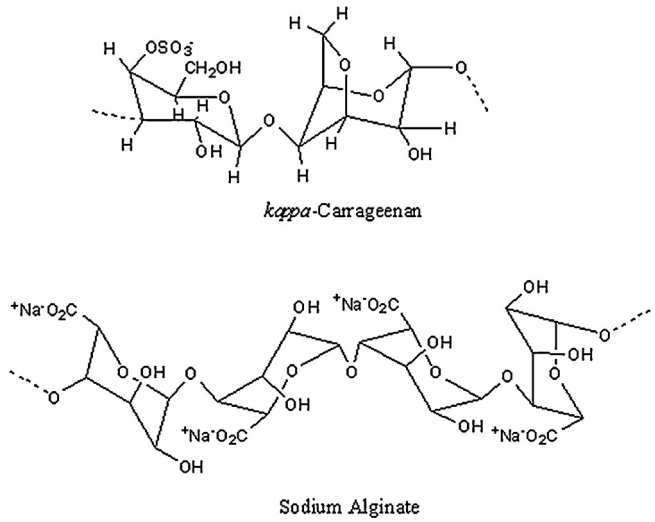

Fig. 1. Structure of *kappa*-carrageenan and sodium alginate.

aqueous solutions (Shawky, 2011). The colors pollutants are anionic or cationic molecules. The existence of anionic and cationic pendants in the hydrogels makes them to show complexing ability with materials with opposite charges. So, anionic and cationic hydrogels have been used to remove anionic and cationic dyes from water (Liu, Zheng, & Wang, 2010; Zhao et al., 2012).

It has been reported that inclusion of nano-clays in the hydrogel composition not only their strength can improve but also the rate and dye adsorption capacity are increased (Liu & Zhang, 2007). Nanocomposite hydrogels containing Na-montmorillonite (Dalaran, Emik, Guclu, Iyim, & Ozgumus, 2009), laponite (Li, Kim, Yoo, & Lee, 2009), attapulgite (Wang & Wang, 2010), and sepiolite (Ekici, Isikver, & Saraydin, 2006) have been synthesized and used to remove pollutions from aqueous solutions.

While the pK_a value of the carboxyl groups of alginate range between 3.4 and 4.4 (Goh et al., 2012), the pK_a of sulfate groups on the carrageenan is lower than that of carboxylate groups (pK_a of methane sulfonic acid is ~−2.0) (Hosseinzadeh et al., 2005). Due to the difference in pK_a values of *kappa*-carrageenan and sodium alginate, we attempt to synthesis nanocomposite hydrogels from binary mixture of these biopolymers by incorporation of Na-MMt nanoclay. Firstly, the nanocomposites containing various amount of Na-MMt and different weight ratios of two biopolymers were synthesized. The obtained nanocomposites were evaluated to remove cationic CV dye from water. The dye adsorption capacity of nanocomposites was studied as a function of clay and biopolymers weight ratio. The experimental data were analyzed according to pseudo first-order and pseudo second-order kinetics, as well as the Freundlich and Langmuir isotherm models. Then, the effect of pH on the dye adsorption capacity of nanocomposites was investigated.

2. Materials and methods

2.1. Materials

kappa-Carrageenan was obtained from Condinson Co. (Denmark). Sodium alginate was purchased from Fluka (Switzerland). MBA crosslinker and APS initiator from Fluka, and acrylamide (AAm) from Rotterdam, The Netherlands, were of analytical grade and were used as received. Natural sodium-montmorillonite (sodium Cloisite, Na-MMt) as a clay with cation exchange capacity of 92 meq./100 g of clay was provided by Southern Clay Products. All other ingredients were analytical grades and were used as received.

2.2. Synthesis of nanocomposites

The nanocomposite hydrogels were synthesized by solution polymerization of acrylamide monomer in the presence of Na-MMt nanoclay and biopolymers. In brief, the Na-MMt clay (0, 0.1, 0.25, 0.5, 0.75, and 1 g) was dispersed in 50 mL of distilled water and stirred under magnetic stirrer for overnight. The dispersed Na-MMt was sonicated for 15 min and adjusted the temperature at 70 °C. Then, 0.5 g of Alg and 0.5 g of Car were added an allowed to complete dissolution. After complete dissolution of biopolymers, the dissolved oxygen was removed using N_2 gas for 30 min. The APS initiator (0.1 g dissolved in 2 mL water) was added and allowed to induce free radicals onto biopolymers for 5 min. Finally, 3 g of AAm and 0.1 g of MBA (dissolved in 2 mL water) were poured into polymerization solution. The produced nanocomposites were cut into small pieces and immersed in excess water to extract the un-reacted components. After purification of nanocomposites for 2 days, the samples were dried at 50 °C for constant weight. The dried samples were ground and passed through a 40-mesh sieve to achieve uniform particle size. The samples were kept away from light and moisture. To study the effect of biopolymers, samples were synthesized as above by varying the ration of biopolymers.

The suffix *m* and *n* in CarAlg/MMt*m* and Car*n*Alg/MMt*m* are weight of clay and percentage of *kappa*-carrageenan in biopolymers feed, respectively. The Car and Alg content in CarAlg/MMt*m* series was the same (0.5 g Car + 0.5 Alg). The MMt content was 0.25 g in Car*n*Alg/MMt*m* series.

2.3. Swelling measurement

Nanocomposite hydrogel samples (0.10 g) were immersed in 100 mL distilled water and allowed to soak for 24 h at room temperature. After this time, they were removed from the water, blotted with filter paper to remove surface water, weighed and the DS (g water/g dried nanocomposite) was calculated using Eq. (1):

$$\mathrm{DS\,(g/g)} = \frac{W_s - W_d}{W_d} \tag{1}$$

where W_s and W_d are the weights of the swollen nanocomposites and the dry sample, respectively.

2.4. Adsorption of CV dye

Dye adsorption was carried out by immersing the 0.05 g of nanocomposites into 50 mL of dye solution with 30 mg L^{-1} of CV. The pH of initial dye solution was 6.4. All adsorption experiments were examined through a batch method on a shaker with a constant speed at 120 rpm. To study the adsorption kinetics, at specified time intervals, the amount of adsorbed CV was evaluated using a UV spectrometer at λ_{max} = 590 nm. The content of adsorbed dye was calculated using following Eq. (2):

$$q_t = \frac{(C_0 - C_t)}{m} \times V \tag{2}$$

where C_0 is the initial CV concentration (mg L^{-1}), C_t is the remaining dye concentration in the solution at time t, V is the volume of dye solution used (L), and m is the weight of nanocomposite (g). Adsorption isotherm was carried out by immersing of 0.05 g of nanocomposites into 50 mL of dye solutions with 10, 20, 30, 50, 70, and 100 mg L^{-1} of CV for 24 h. The pH of initial dye solutions was varied from 6.3 for solution with 10 ppm of CV to 6.85 for solution with 100 ppm of CV. The equilibrium adsorption capacity of nanocomposites, q_e (mg L^{-1}), was determined using Eq. (2). At this equation, the C_t and the q_t will be replaced with equilibrium concentration of dye in the solution (C_e) and equilibrium adsorption capacity (q_e), respectively.

The removal efficiency (RE, %) of CV by nanocomposites was calculated as bellows:

$$\text{RE } (\%) = \frac{C_0 - C_e}{C_0} \times 100 \quad (3)$$

where C_e is the remaining CV concentration in the solution.

For investigation the effect of pH of initial dye solutions on adsorption capacity of nanocomposites, samples were immersed in dye solution with the desired pHs. The adjustment of pH was carried out using 0.1 M of HCl and NaOH solution.

2.5. Instruments

Dried samples were coated with a thin layer of gold and imaged in a SEM instrument (Vega, Tescan). One-dimensional, wide angle X-ray diffraction patterns were obtained by using a Siemens D-500 X-ray diffractometer with wavelength, $\lambda = 1.54$ Å (Cu-Kα), at a tube voltage of 35 kV, and tube current of 30 mA. TEM micrographs were recorded with a Philips CM10 operating at 60 kV tension.

3. Results and discussion

3.1. Synthesis and characterization

Solution polymerization was used to synthesize of nanocomposite hydrogels by grafting of AAm onto binary mixture of *kappa*-carrageenan and sodium alginate biopolymers using sodium montmorillonite nanoclay. MBA and APS were used as crosslinker and initiator, respectively. The characteristic graphs of CarAlg/MMt nanocomposites from XRD, TEM, and SEM studied are illustrated in Fig. 2. Fig. 2a indicates the XRD patterns of neat clay and nanocomposites containing 0.25 and 0.5 g of Na-MMt nanoclay (CarAlg/MMt0.25, CaraAlg/MMt0.5). The XRD profile of pristine Na-MMt imply a strong diffraction peak at $2\theta = 7.6^\circ$ corresponding to the distance of clay sheets with d spacing 11.61 Å. After polymerization reaction, the sharp peak of nanoclay at $2\theta = 7.6^\circ$ was disappeared and may be attributed to completely exfoliation of Na-MMt nanoclay in nanocomposite matrix. But, because of strong noises in XRD profiles of nanocomposites, it was difficult to conclude the exfoliation or intercalation of Na-MMt nanoclay in polymer matrix. So, we investigated the TEM image of CarAlg/MMt0.25 and the result was shown in Fig. 2b. The dark and thin lines corresponded to Na-MMt layers. It can be seen that Na-MMt layers were obtained and indicates that the clay layers exists in exfoliated type.

One of the most crucial properties of nanocomposites which can be considered is hydrogel microstructure morphology. Fig. 2c–e shows the SEM micrographs of clay-free hydrogel (CarAlg), CarAlg/MMt0.25, and CarAlg/MMt0.0.5 nanocomposites. While the hydrogel without clay showed a relatively tight and smooth surface (Fig. 2c), the nanocomposites (Fig. 2d and e) contain coarse, undulant, and relatively porous surface. Also, according to SEM images, the porosity of nanocomposites was slightly enhanced as the Na-MMt was increased. This observation is similar as our previous works using Na-MMt as nanoclay to synthesize of *kappa*-carrageenan based nanocomposite hydrogels (Mahdavinia, Massoudi, Baghban, & Massoumi, 2012; Mahdavinia, Massoumi, Jalili, & Kiani, 2012; Mahdavinia & Zhalebaghy, 2012).

3.2. Dye adsorption study

3.2.1. Kinetic of dye adsorption

Adsorption kinetic as a useful information on the rate of dye adsorption can consider as an important factor to proper design of adsorbent (Liu, Gao, et al., 2010). So, the adsorption kinetic was investigated to measure the required equilibrium time of adsorption of CV dye onto samples. The adsorption of CV dye on the samples was examined for 8 h and the results are shown in Fig. 3a. Initially, the adsorption of dye onto hydrogels sharply increases and then begins to level off. The equilibrium dye adsorption was achieved after ~2 h. It is clear from figure that by introducing of Na-MMt clay in CarAlg hydrogels, the dye adsorption capacity was slightly increased. Furthermore, from the initial slope of the curves, the speed of dye adsorption was enhanced as the clay amount increased in hydrogel composition. According to SEM graphs, the introducing of Na-MMt nanoclay into CarAlg composition caused a loose and porous surface. The increment in the rate of dye adsorption onto nanocomposites can be attributed to the increase in the active centers due to porosity. Also, a slightly enhancement in dye adsorption capacity of nanocomposites may be attributed to the high degree of swelling (DS, Table 1) and porosity of nanocomposites. A similar observation for the adsorption of cationic dye onto chitosan-g-poly (acrylic acid)/MMt nanocomposites have been reported by Wang, Zhang, and Wang (2008). In fact, the increase in both DS and porosity was affected the adsorption capacity and rate of dye onto adsorbents. During 2 h, the removal efficiency for CarAlg hydrogel and CarAlg/MMt0.25 nanocomposite was obtained 66.7 and 80.3%, respectively. This result indicates the improvement of dye adsorption speed of CarAlg hydrogel by introducing of Na-MMt. Also, while the removal efficiency of CarAlg at equilibrated time was obtained 90.3%, the removal efficiency for CarAlg/MMt series was obtained up to 99%.

For a more detailed study, we endeavored to examine the dye adsorption onto hydrogels containing only 25 wt% of carrageenan (Car/PAAm), alginate (Car/PAAm), and sodium montmorillonite (Na-MMt/PAAm). The hydrogels were immersed into 50 mL of CV solutions with 30 ppm concentration and pH = 6.4. The results are shown in Fig. 3b. According to the data, the adsorption capacity of hydrogels was not significant. But, from the initial slope of dye adsorption profiles, the rate of dye adsorption onto hydrogel containing 25 wt% of Na-MMt was obtained higher that the other hydrogels. From this observation it may be concluded that the main factor in the rate of dye adsorption in CarAlg/MMt nanocomposite is porosity due to the inclusion Na-MMt into hydrogel composition.

Pseudo first-order and pseudo second-order kinetic models were examined to obtain rate constant and equilibrium adsorption capacity for nanocomposites. Kinetic data were analyzed by using the pseudo first-order equation as below (Dai et al., 2011):

$$\ln(q_e - q_t) = \ln q_{e1} - k_1 t \quad (4)$$

where q_e and q_t (mg g^{-1}) are the amount of adsorbed dye on the nanocomposites at equilibrium and at time t, respectively. k_1 (min^{-1}) presents the rate constant of first-order adsorption. q_{e1} indicates the theoretically equilibrium adsorption. In order to obtain model calculations k_1, q_{e1}, and R^2 (correlation coefficient), we can plot $\ln(q_e - q_t)$ against t for pseudo first-order.

Also, kinetic data were analyzed by using the pseudo-second-order equation as below (Dai et al., 2011):

$$\frac{t}{q_t} = \frac{1}{k_2 (q_{e2})^2} + \frac{t}{q_{e2}} \quad (5)$$

here k_2 (g mg^{-1} min^{-1}) is rate constant of second-order adsorption and q_{e2} is the theoretical adsorbed dye (mg g^{-1}) that can be calculated from pseudo second-order. In order to obtain model calculations k_2 and theoretically equilibrium adsorption (q_{e2}) as well as R^2 (correlation coefficient), we can t/q_t against t (Fig. 3c). Model calculations for all nanocomposites were given in Table 1. It was found that the plotting of t/q_t against t gives a straight-line with a high correlation coefficient ($R^2 > 0.97$) and it can be concluded that adsorption kinetic of dye by all nanocomposites has the best fitting to the pseudo second-order. As can be seen from the data,

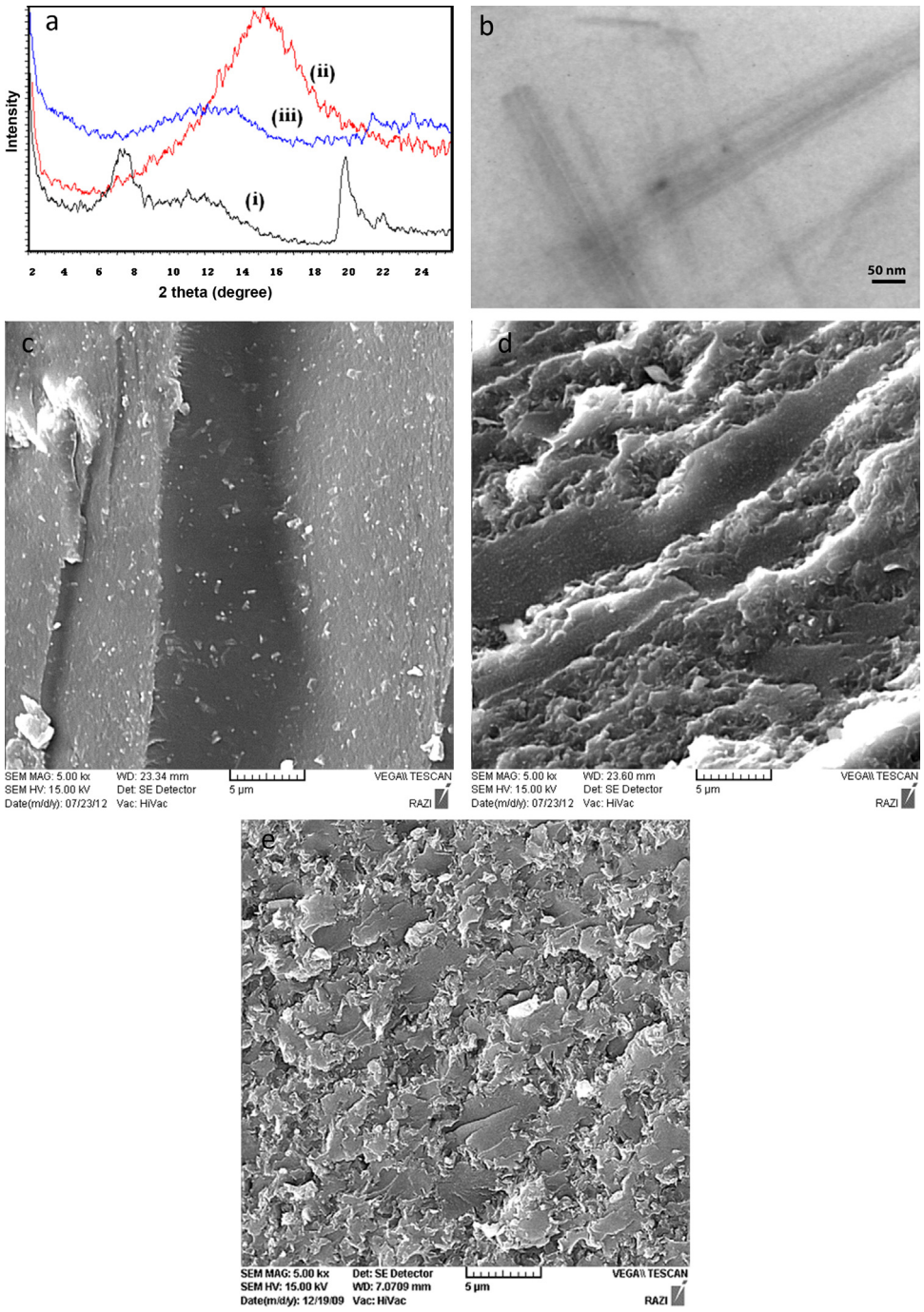

Fig. 2. (a) XRD pattern of pristine Na-MMt (i), nanocomposites CarAlg/MMt0.25 (ii), and CaraAlg/MMt0.5 (iii); (b) TEM graph of CarAlg/MMt0.25 nanocomposite; SEM image of (c) CarAlg clay-free hydrogel; (d) CarAlg/MMt0.25; and (e) CarAlg/MMt0.5 nanocomposites.

Table 1
Kinetic parameters for the adsorption of CV onto nanocomposites according to pseudo-first-order and pseudo-second-order kinetics; degree of swelling (DS) of nanocomposites by varying MMt content.

	First-order kinetic			Second-order kinetic			q_e, Exp., mg g^{-1}	DS, g/g
	$k_1 \times 10^3$, min^{-1}	R^2	q_{e1}, mg g^{-1}	$k_2 \times 10^4$, g mg^{-1} min^{-1}	R^2	q_{e2}, mg g^{-1}		
CarAlg	6.4	0.82	21	4.13	0.99	31	27.1	16.2
CarAlg/MMt0.1	7.7	0.93	22.4	4.86	0.99	32	28.4	18.5
CarAlg/MMt0.25	8.5	0.89	17.8	8.7	0.99	31.3	29.1	22.7
CarAlg/MMt0.5	6.3	0.88	18.3	5.1	0.99	32.7	29.1	23
CarAlg/MMt0.75	5.2	0.7	18.5	14.6	0.98	28.9	29.7	18.5
CarAlg/MMt1	5	0.74	18.6	13.4	0.97	28.81	29.7	15.3

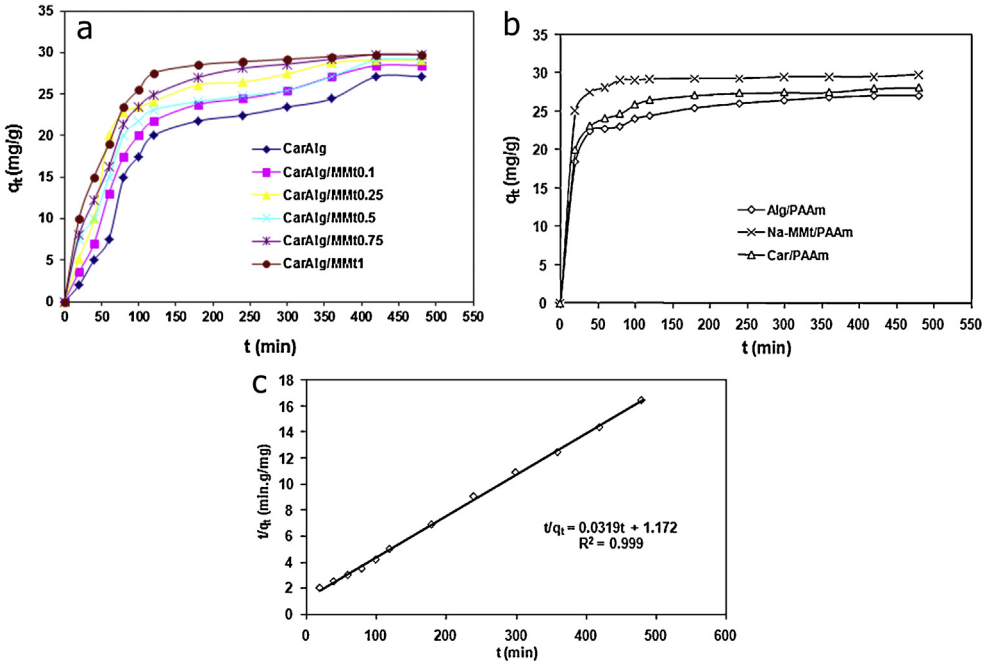

Fig. 3. (a) Kinetics of CV removal by CarAlg/MMt nanocomposites with different clay content (C_0: 30 mg L^{-1}, pH: 6.4, adsorbent dosage: 50 mg/50 mL, RPM: 120, T: RT); (b) kinetics of CV removal by Car/PAAm, Alg/PAAm, and Na-MMt/PAAm hydrogels (C_0: 30 mg L^{-1}, pH: 6.4, adsorbent dosage: 50 mg/50 mL, RPM: 120, T: RT); and (c) plotting of t/q_t against t according to second order kinetic for CarAlg/MMt0.25 nanocomposite.

according to pseudo second-order kinetic, the theoretical equilibrium adsorption capacities are in agreement with the experimental data.

3.2.2. Adsorption isotherm

Adsorption isotherm can be considered as an essential necessity to design of adsorption system. In the adsorption isotherm studies, the hydrogels were immersed into dye solutions with different initial concentration ranging from 10 to 100 mg L^{-1}. The adsorption capacity of hydrogels was calculated at equilibrium time. Fig. 4a shows the effect of initial dye concentration on the adsorption capacity of CarAlg/MMt0.25. As the initial dye concentration was increased, the adsorption capacity of sample was enhanced and then switches to level off. At higher initial concentration, the adsorption sites reach on saturation state and the adsorption remains constant.

The Langmuir and Freundlich isotherm models can be applied to analysis of experimentally equilibrium data from adsorption of dye onto samples at equilibrium time. In the Langmuir adsorption model, adsorption of adsorbate takes place at specific homogeneous sites within the adsorbent and valid for monolayer adsorption onto adsorbents (Kasgoz & Durmus, 2008). The expression of the applied Langmuir model is given by Eq. (6):

$$\frac{C_e}{q_e} = \frac{C_e}{q_m} + \frac{1}{q_m b} \tag{6}$$

where C_e is the equilibrium dye concentration in the solution (mg L^{-1}), b is the Langmuir adsorption constant (L mg^{-1}), and q_m is the theoretical maximum adsorption capacity (mg g^{-1}). The q_m and b can be calculated from the slope and intercept of a linear plot of C_e/q_e versus C_e, respectively (Fig. 4b).

In the Freundlich model, the adsorption of adsorbate occurs on a heterogeneous surface by multilayer sorption and the adsorption capacity can increase with an increase in adsorbate concentration (Kasgoz & Durmus, 2008). Freundlich isotherm is represented by the following equation:

$$\ln q_e = \ln k_f + \frac{1}{n} \ln C_e \tag{7}$$

where k_f is the equilibrium adsorption coefficient (mg$^{(1-n)}$ L^n g^{-1}), and $1/n$ is the empirical constant. The k_f and n values for nanocomposites can be achieved from the intercept and the slope of plotting $\ln q_e$ against $\ln C_e$. In fact, the n value depicts the favorability of adsorption process and k_f is the adsorption capacity and intensity of the adsorbate.

The all expressions in Langmuir and Freundlich equations and equilibrated adsorption of all nanocomposites were calculated according to experimental data and summarized in Table 2. In accordance the high correlation coefficient in Langmuir equation ($R^2 > 0.91$), it depicts that Langmuir isotherm is the best fit of experimental data than the Freundlich model. From Langmuir parameters, the theoretical and experimental maximum adsorption capacities of hydrogels are in agreement and confirming the best fit of Langmuir model with practical data. The experimental q_m values ($q_{m,exp}$) of the hydrogels from isotherm studies was shown in Fig. 4c. While the q_e values from kinetic study were not significant, the adsorption capacity of samples was affected by the initial dye concentration. The $q_{m,exp}$ values were obtained by immersing of 0.05 g of hydrogels into 50 mL of dye solution with 100 mg g^{-1} concentration at pH = 6.85. The $q_{m,exp}$ values for nanocomposites were in agreement with the swelling capacity of hydrogels. In fact, by the increasing of Na-MMt content up to 0.5 g not only the swelling capacity was increased, but also according to the SEM graphs the porosity was relatively enhanced. So, the increase in $q_{m,exp}$ values can be attributed to the increase in both DS and porosity of hydrogels. The more increase in the MMt content caused a decrease in swelling capacity and subsequently the $q_{m,exp}$ values were decreased. According to experimental data, the maximum adsorption capacity (88.8 mg g^{-1}) was obtained for CarAlg/MMt0.5 sample (pH = 6.85, concentration of CV 100 mg L^{-1}).

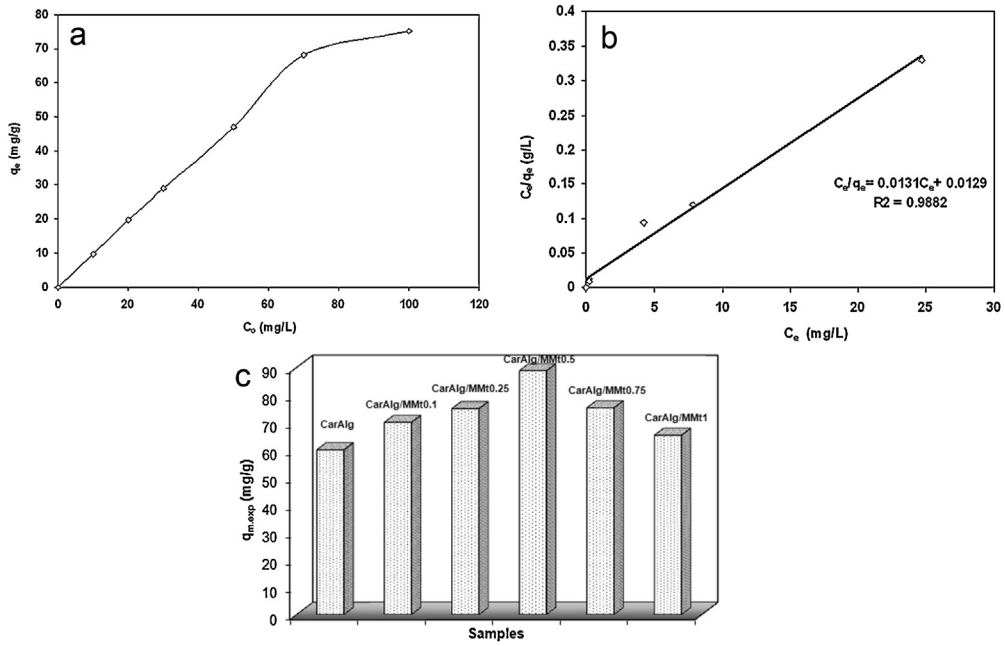

Fig. 4. (a) Effect of initial dye concentration of the adsorption capacity of CarAlg/MMt0.25 nanocomposite (pH: 6.3–6.85, adsorbent dosage: 50 mg/50 mL, RPM: 120, T: RT); (b) plotting of C_e/q_e against C_e according to Langmuir model for CarAlg/MMt0.25 nanocomposite; and (c) maximum dye adsorption capacity of nanocomposites ($q_{m,exp}$) according to experimental data.

The favorability of the adsorption (R_L) was evaluated from parameters of Langmuir adsorption isotherm model. The R_L can calculate from the following equation (Auta & Hameed, 2011):

$$R_L = \frac{1}{1 + bC_0} \tag{8}$$

where b is the Langmuir constant ($L\,mg^{-1}$) and C_0 is the initial concentration of dye. The R_L can vary: for $R_L > 1$ the adsorption is unfavorable; $R_L = 1$ the adsorption is Linear condition; the adsorption is favorable when $0 < R_L < 1$; and $R_L = 0$ is for irreversible conditions. According to Table 2, the R_L values for hydrogels were achieved between 1 and zero indicating favorable adsorption of CV onto obtained hydrogel nanocomposites.

3.2.3. Effect of pH on the adsorption

Removal of adsorbate from aqueous solution onto adsorbent is influenced by the pH of pollutant solution. In fact, by the changing the pH of solution, the nature of active center on the adsorbent can change and finally affect the adsorption behavior of adsorbate. The CarAlg/MMt nanocomposites comprise *kappa*-carrageenan, sodium alginate, polyacrylamide, and sodium montmorillonite components. Among them, polyacrylamide is non-ionic and pH-independent. *kappa*-Carrageenan is an ionic polysaccharide comprising sulfate groups ($-OSO_3^-$). These pendants are completely dissociated in the overall pH range and the hydrogels from this biopolymer shows pH-independent swelling behavior (Durmaz & Okay, 2000). In fact, in the overall pH range, these anionic groups are in dissociation form. While the sulfate groups on the carrageenan are pH-independent, the carboxylate pendants on the alginate biopolymer are pH-dependent and the pH of solution can affect the dissociation of these anionic centers. The sodium montmorillonite nanoclay comprises anionic centers on its surface. These anionic centers can accept proton and so, the adsorption of dye onto montmorillonite can vary by changing the pH of initial dye solution.

Fig. 5 shows the effect of pH of initial dye solution on the adsorption of CV onto nanocomposite hydrogels containing different amount of Na-MMt and biopolymers ratio. According to Fig. 5a, not only the dye adsorption capacity of nanocomposite hydrogels is pH-dependent, but also the clay content can affect the dye adsorption capacity of samples at acidic media. When the pH of dye solution was adjusted at pH = 2–4, a reduction in dye adsorption capacity was occurred and this behavior can be attribute to: (a) competition between cationic dye and H^+ in adsorbing onto anionic centers of nanocomposites and (b) the protonization of carboxylate groups on alginate and anionic centers of Na-MMt. Under acidic condition, an enhancement in dye adsorption capacity of hydrogels was observed by increasing the clay content in hydrogel composition. It has been reported that the adsorption of cationic dye onto sodium montmorillonite is decreased at acidic pHs (Selvam et al., 2008). In this study, the adsorption of CV onto nanocomposites was increased as the clay content was increased. In fact, by

Table 2
Langmuir and Freundlich isotherm model parameters for adsorption of CV onto nanocomposites.

	Freundlich model			Langmuir model				$q_{m,exp}$
	n, g L^{-1}	K_f, $mg^{(1-n)}\,L^n\,g^{-1}$	R^2	q_m, mg g^{-1}	b, L mg^{-1}	R^2	R_L	
CarAlg	2.59	15.5	0.09032	66.7	0.17	0.992	0.37	60
CarAlg/MMt0.1	1.77	15.5	0.8318	85.2	0.35	0.9222	0.28	70.1
CarAlg/MMt0.25	2.2	27.8	0.8542	83.3	0.5	0.9183	0.16	75.2
CarAlg/MMt0.5	2.14	26.8	0.9064	80	0.73	0.9358	0.12	88.8
CarAlg/MMt0.75	3.31	24	0.5562	76.3	1.01	0.9882	0.09	75.3
CarAlg/MMt1	3.47	28.7	0.8446	66.7	1.61	0.9982	0.05	65.3

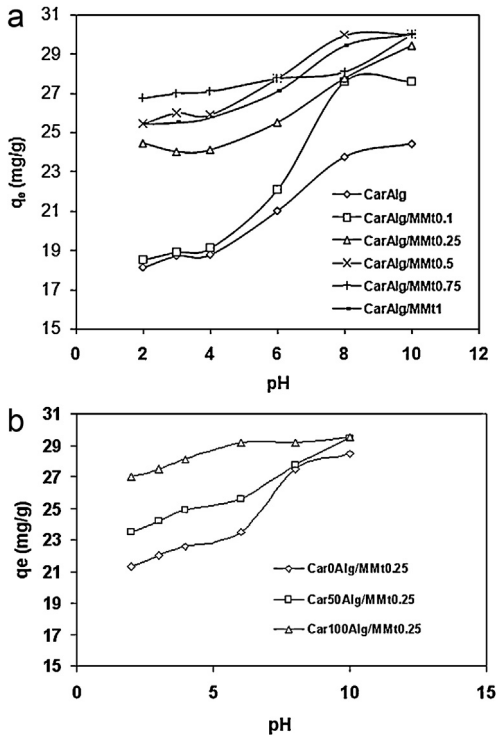

Fig. 5. Effect of pH on the dye adsorption capacity of nanocomposites containing (a) different content of clay and (b) different ratio of biopolymers.

increasing the clay content, the active center for dye adsorption was enhanced.

The pK_a values for two biopolymers are not similar. The pK_a of sulfate groups on *kappa*-carrageenan is lower than the carboxylate groups on sodium alginate. So, we tried to study the effect of pH on the dye adsorption capacity of nanocomposite as a function of two biopolymers ratio. The results are shown in Fig. 5b. As can be seen from figure, under acidic condition, the dye adsorption capacity of nanocomposite depends on the weight ratio of two biopolymers. The nanocomposite containing sodium alginate component adsorbs low content of dye. This can be attributed to convert of anionic carboxylate groups ($-CO_2^-$) to carboxylic form ($-CO_2H$) and subsequently dye adsorption capacity is decreased. By introducing of *kappa*-carrageenan in nanocomposite composition, the dye adsorption capacity of nanocomposite was improved that can be attributed to the presence of dissociated sulfate groups on *kappa*-carrageenan. When the pH of dye solution was raised from 4 to 6, while the slope of changing in dye adsorption capacity of nanocomposite containing carrageenan was relatively low, the changing in dye adsorption capacity of nanocomposites containing alginate was sharp. The increment in dye adsorption of these nanocomposites can be attributed to convert of carboxylic to carboxylate groups. Also, the effect of biopolymer ratio on the dye adsorption speed of nanocomposites at pH = 2 was studied. According to Fig. 6 and initial slope of curves, the dye uptake by Car100Alg/MMt0.25 was higher than that of Car0Alg/MMt0.25 hydrogel. This high speed of dye adsorption can be attributed to the dissociated sulfate groups on the carrageenan in acidic media.

3.2.4. Desorption study

To evaluate the possibility of reusing of CarAlg/MMt nanocomposite hydrogels over multiple cycles, desorption of adsorbed dye was examined using various solutions. The desorption in distilled water, 0.1 M HCl, and 0.1 M NaOH was lower than 12% of adsorbed dye. The 0.5 M KCl solutions were used to desorption studies. When the 0.5 M KCl in water was contacted with samples containing

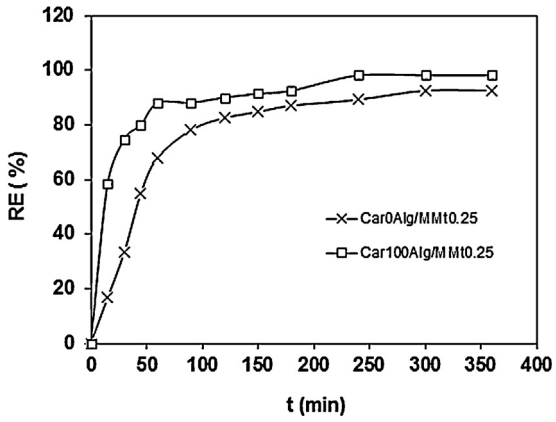

Fig. 6. Effect of biopolymer weight ratio on the dye removal efficiency and speed at pH = 2.

adsorbed dye, the desorption efficiency was about 25%. But, when the 0.5 M KCl solution in ethanol/water (50/50, V/V) was used, desorption was reached up to 75%. It may be noted that desorption efficiency for CarAlg hydrogel in the 0.5 M KCl solution in 50:50 of ethanol/water was more than 95%. In fact, while the introducing of Na-MMt nanoclay was improved the dye adsorption capacity of CarAlg hydrogel, desorption was lower than the clay-free hydrogel.

4. Conclusions

A novel nanocomposite hydrogel was synthesized from grafting of acrylamide onto binary mixture of *kappa*-carrageenan and sodium alginate biopolymers by incorporation of Na-MMt nanoclay. The structure and morphology of nanocomposites were characterized using XRD, TEM, and SEM techniques. The XRD and TEM results showed exfoliated Na-MMt sheets in hydrogel matrix. According to the SEM micrographs, inclusion of Na-MMt into CarAlg hydrogel caused a coarse surface. The obtained nanocomposites were used to adsorb cationic CV dye from water. As compared to clay-free hydrogel (CarAlg), the CarAlg/MMt nanocomposite hydrogels exhibit high adsorption speed and capacity. The slightly increment in dye adsorption capacity was because of porous structure of nanocomposites. The results showed that the pseudo second-order adsorption kinetic was predominated for the adsorption of CV onto hydrogels. Langmuir model was obtained as the best model for the adsorption of CV onto hydrogels and maximum adsorption capacity from Langmuir isotherm was obtained 85 mg g^{-1}. The effect of pH of initial dye solution on the adsorption revealed that the dye adsorption capacity of hydrogels is influenced by both clay content and biopolymers weight ratio. At acidic media, the dye adsorption capacity of nanocomposites was enhanced as the carrageenan and clay content were increased in nanocomposite composition.

References

Auta, M., & Hameed, B. H. (2011). Preparation of waste tea activated carbon using potassium acetate as an activating agent for adsorption acid blue 25 dye. *Chemical Engineering Journal, 171*, 502–509.

Bajpai, S. K., & Tankhiwale, R. (2006). Investigation of water uptake behavior and stability of calcium alginate/chitosan bi-polymeric beads: Part-1. *Reactive and Functional Polymers, 66*, 645–658.

Crini, G. (2005). Recent developments in polysaccharide-based materials used as adsorbents in wastewater treatment. *Progress in Polymer Science, 30*, 38–70.

Dai, J., Yang, H., Yan, H., Shangguan, Y., Zheng, Q., & Cheng, R. (2011). Phosphate adsorption from aqueous solutions by disused adsorbents: Chitosan hydrogel beads after the removal of copper (II). *Chemical Engineering Journal, 166*, 970–977.

Dalaran, M., Emik, S., Guclu, G., Iyim, T. B., & Ozgumus, S. (2009). Removal of acidic dye from aqueous solutions using poly(DMAEMA-AMPSHEMA)terpolymer/MMT nanocomposite hydrogels. *Polymer Bulletin, 63*, 159–171.

Datta, S., Mody, S., Gopalsamy, G., & Jha, B. (2011). Novel application of *k*-carrageenan: As a gelling agent in microbiological media to study biodiversity of extreme alkaliphile. *Carbohydrate Polymers*, *85*, 465–468.

Dragan, E. S., Perju, M. M., & Dinu, M. V. (2012). Preparation and characterization of IPN composite hydrogels based on polyacrylamide and chitosan and their interaction with ionic dyes. *Carbohydrate Polymers*, *88*, 270–281.

Durmaz, S., & Okay, O. (2000). Acrylamide/2-acrylamido-2-methylpropane sulfonic acid sodium salt-based hydrogels: Synthesis and characterization. *Polymer*, *41*, 3693–3704.

Ekici, S., Isikver, Y., & Saraydin, D. (2006). Poly(acrylamide-sepiolite) composite hydrogels: Preparation, swelling and dye adsorption properties. *Polymer Bulletin*, *57*, 231–241.

Goh, C. H., Heng, P. W. S., & Chan, L. W. (2012). Alginates as a useful polymer for microencapsulation and therapeutic application. *Carbohydrate Polymers*, *88*, 1–12.

Hosseinzadeh, H., Pourjavadi, A., Mahdavinia, G. R., & Zohuriaan-Mehr. (2005). Modified carrageenan. 1. H-CarragPAM, a novel biopolymer-based superabsorbent hydrogel. *Journal of Bioactive and Compatible Polymers*, *20*, 475–490.

Kasgoz, H., & Durmus, A. (2008). Dye removal by a novel hydrogel-clay nanocomposite with enhanced swelling properties. *Polymers for Advanced Technologies*, *19*, 838–845.

Li, P. S., Kim, N. H., Yoo, G. H., & Lee, J. H. (2009). Poly(acrylamide/laponite) nanocomposite hydrogels: Swelling and cationic dye adsorption properties. *Journal of Applied Polymer Science*, *111*, 1786–1798.

Liu, P., & Zhang, L. (2007). Adsorption of dyes from aqueous solutions or suspensions with clay nano-adsorbents. *Separation and Purification Technology*, *58*, 32–39.

Liu, Y., Gao, X., Hua, R., Wang, Y., Liu, Y., Pang, C., et al. (2010). Selective adsorption of uranyl ion on ion-imprinted chitosan/PVA crosslinked hydrogel. *Hydrometallurgy*, *104*, 150–155.

Liu, Y., Zheng, Y., & Wang, A. (2010). Enhanced adsorption of Methylene Blue from aqueous solution by chitosan-*g*-poly(acrylic acid)/vermiculite hydrogel composites. *Journal of Environmental Science*, *22*, 486–493.

Mahdavinia, G. R., Massoudi, A., Baghban, A., & Massoumi, B. (2012). Novel carrageenan-based hydrogel nanocomposites containing laponite RD and their application to remove cationic dye. *Iranian Polymer Journal*, *21*, 609–619.

Mahdavinia, G. R., Massoumi, B., Jalili, K., & Kiani, G. R. (2012). Effect of sodium montmorillonite nanoclay on the water absorbency and cationic dye removal of carrageenan-based nanocomposite superabsorbents. *Journal of Polymer Research*, *19*, 9947.

Mahdavinia, G. R., & Zhalebaghy, R. (2012). Removal kinetic of cationic dye using poly (sodium acrylate)-carrageenan/Na-montmorillonite nanocomposite superabsorbents. *Journal of Materials and Environmental Science*, *3*, 895–906.

Mohamadnia, Z., Zohuriaan-Mehr, M. J., Kabiri, K., Jamshidi, A., & Mobedi, H. (2008). Ionically crosslinked carrageenan-alginate hydrogel beads. *Journal of Biomaterials Science, Polymer Edition*, *19*, 47–59.

Nair, L. S., & Laurencin, C. T. (2007). Biodegradable polymers as biomaterials. *Progress in Polymer Science*, *32*, 762–798.

Nochos, A., Douroumis, D., & Bouropolos, N. (2008). In vitro release of bovine serum albumin from alginate/HPMC hydrogel beads. *Carbohydrate Polymers*, *74*, 451–457.

Omidian, H., Rocca, J. G., & Park, K. (2005). Advances in super-porous hydrogels. *Journal of Controlled Release*, *102*, 3–12.

Pawar, S. N., & Edgar, K. J. (2012). Alginate derivatization: A review of chemistry, properties and applications. *Biomaterials*, *33*, 3279–3305.

Piculell, L. (1995). Gelling carrageenans. In A. M. Stephen (Ed.), *Food polysaccharides and their applications* (pp. 205–217). New York: Marcel Dekker.

Pourjavadi, A., Barzegar, Sh., & Mahdavinia, G. R. (2006). MBA-crosslinked Na-Alg/CMC as a smart full-polysaccharide superabsorbent hydrogels. *Carbohydrate Polymers*, *66*, 386–395.

Selvam, P. P., Preethi, S., Basakaralingam, P., Thinakaran, N., Sivasamy, A., & Sivanesan, S. (2008). Removal of rhodamine B from aqueous solution by adsorption onto sodium montmorillonite. *Journal of Hazardous Materials*, *155*, 39–44.

Shawky, H. A. (2011). Improvement of water quality using alginate/montmorillonite composite beads. *Journal of Applied Polymer Science*, *119*, 2371–2378.

Shen, C., Shen, Y., Wen, Y., Wang, H., & Liu, W. (2011). Fast and highly efficient removal of dyes under alkaline conditions using magnetic chitosan-Fe(III) hydrogel. *Water Research*, *45*, 5200–5210.

Tang, Y., Wang, X., Li, Y., Lei, M., Du, Y., Kennedy, J. F., et al. (2010). Production and characterisation of novel injectable chitosan/methylcellulose/salt blend hydrogels with potential application as tissue engineering scaffolds. *Carbohydrate Polymers*, *82*, 833–841.

Wang, A., & Wang, W. (2010). Nanocomposite of carboxymethyl cellulose and attapulgite as a novel pH-sensitive superabsorbent: Synthesis, characterization and properties. *Carbohydrate Polymers*, *82*, 83–91.

Wang, L., Zhang, J., & Wang, A. (2008). Removal of methylene blue from aqueous solution using chitosan-*g*-poly (acrylic acid)/montmorillonite superadsorbent nanocomposite. *Collides Surface A*, *322*, 47–53.

Zhao, S., Zhou, F., Li, L., Cao, M., Zuo, D., & Liu, H. (2012). Removal of anionic dyes from aqueous solutions by adsorption of chitosan-based semi-IPN hydrogel composites. *Composites Part B: Engineering*, *43*, 1570–1578.